

Supplementary Information

Experiments and Computations of Microfluidic Liquid-Liquid Flow Patterns

Pierre Desir^{δ,a}, Tai-Ying Chen^{δ,a}, Mauro Braconci^c, Basudeb Saha^b, Matteo Maestri^c, and
Dionisios G. Vlachos^{a,b,*}

^aDepartment of Chemical and Biomolecular Engineering, University of Delaware, 150 Academy Street, Newark, Delaware 19716, United States

^bCatalysis Center for Energy Innovation, 221 Academy Street, Newark, Delaware 19716, United States

^cLaboratory of Catalysis and Catalytic Processes, Dipartimento di Energia, Politecnico di Milano, via La Masa 34, 20156 Milano, Italy

^δThese authors contributed equally.

*Corresponding author; vlachos@udel.edu (D.G. Vlachos)

Mesh Convergence Analysis

Different mesh sizes are employed to carry out mesh independence analysis. The mesh is purely hexaedral characterized by grading towards the wall. In particular, the cell size at the wall of the channel is half of that at the middle section. The number of cells per inner diameter (N) employed are 10, 20, 30, 40 and 50, resulting in 29000, 232000, 783000, 1856000 and 3625000 cells, respectively. Convergence is achieved when the water slug length and the velocity profile at the middle of downstream microchannel are mesh-independent. Figure S1 shows the slug length with respect to mesh discretization. Figure S2 shows the parabolic velocity profile in the downstream channel. A mesh with 40 cells is sufficient to achieve mesh convergence for both properties. Analogous results have been reached for all other conditions investigated.

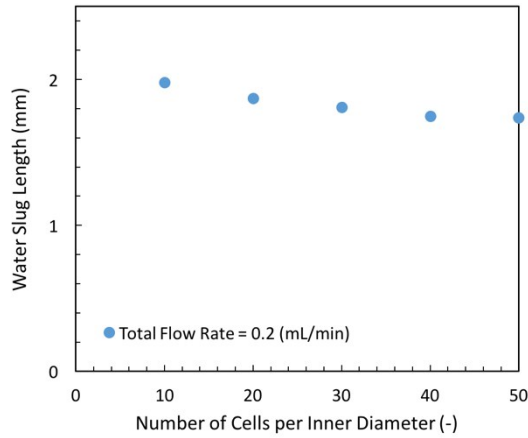


Figure S1. Water slug length with respect to different mesh sizes.

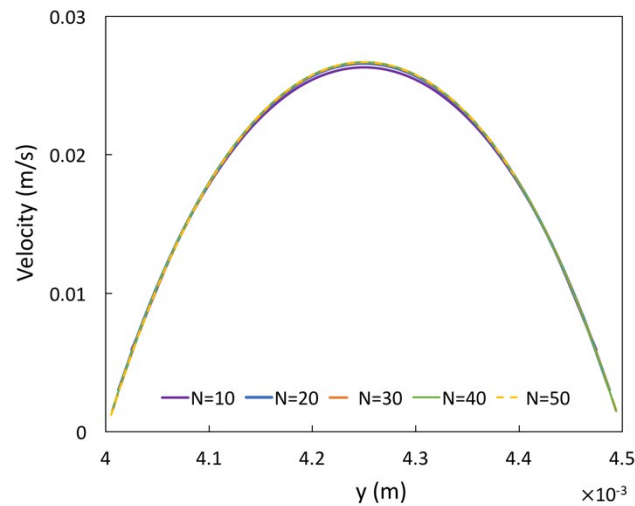


Figure S2. Velocity profile in the downstream channel for different mesh densities.

Internal Structure of T-junction

The T-junction was cut through its middle plane in two halves, which are shown in Figure S3. The center of the top-half is flat and does not contain the internal T-structure. The internal T-structure is embedded in the bottom-half. To further confirm the cross-section of the internal T-structure, an agarose hydrogel replicate of the T-junction is made for visualization using the confocal microscope. The agarose hydrogel mold was dyed with sodium fluorescein to perform a z-stack imaging of the internal T-structure and reconstruct the 3D geometry of the cross-section in ImageJ. The mold was further cut at the edge of one of the branches of the internal T-structure and

placed directly above a 10X objective lens for visualization. Figure S4 shows the 3D reconstruction of the branch of the internal T-structure where the x-y plane shows the edge of the tee branch along with a small section of the non-embedded/flat part of the T-junction while the y-z plane is the 2D projection of the cross-section. From the projected surface, we confirm that the cross-section of the internal T-structure is 500 μm square.

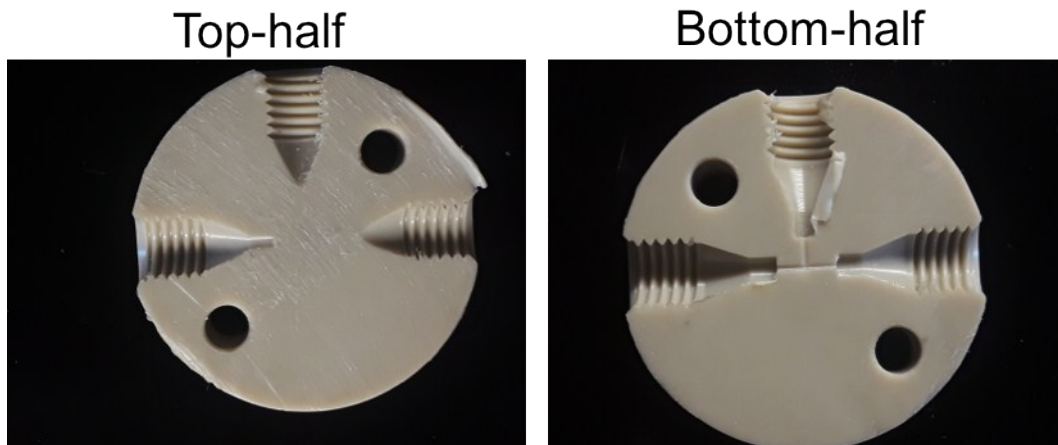


Figure S3. The internal structure of T-junction.

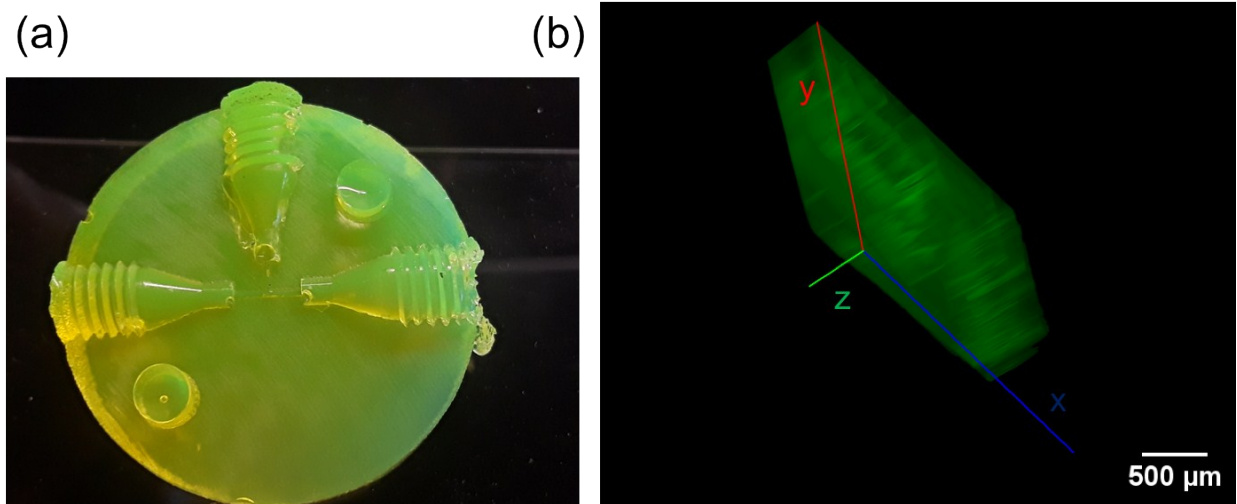


Figure S4. Replicate of T-junction made of agarose hydrogel with dissolved fluorescein (a). The 3D projection of the z-stack imaging from cut of agarose hydrogel mold (b).

Illustration of a Decision Tree

A illustration of a simple decision tree is shown in Figure S5. In Figure S5, there are originally three different flow patterns in the dataset. The algorithm would first separate them into two different subsets using certain criteria for a certain feature (i.e., $Q \geq Q_1$) based on the Gini impurity. Then, it would again separate each subset into the other two different subsets using other criteria and features (i.e., $Org/Aq \geq R_1$). This process is repeated on each subset recursively to build a decision tree until reaching the stopping criteria, i.e., every subset contains only one unique flow pattern.

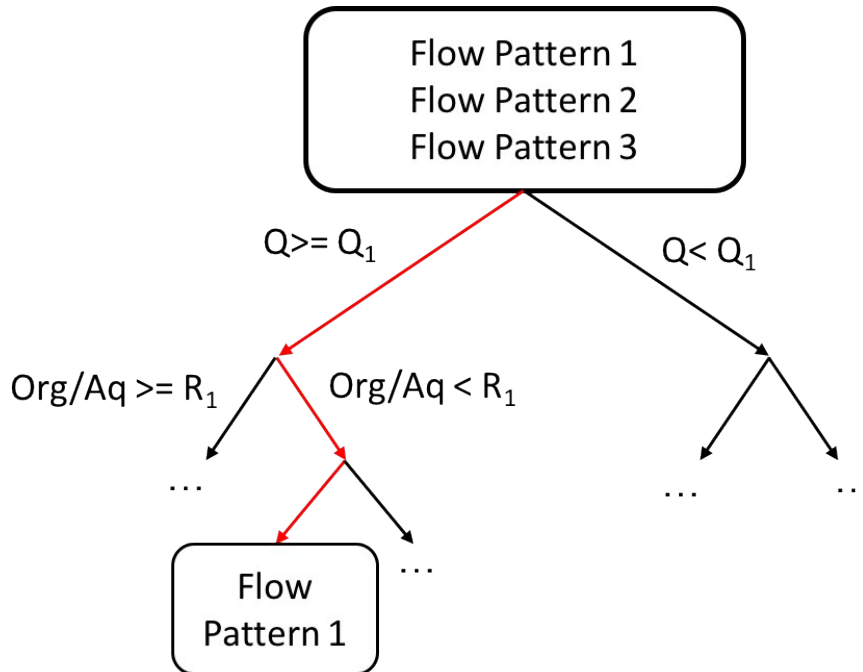


Figure S5. The illustration of a simple decision tree.

Decision Tree Model for Flow Pattern Prediction

The full decision tree model is shown in Figure S6. Different colors represent different classes of flow patterns, and the transparency of the colors represent the ‘purity’ of that set of data. When the transparency is zero, there is only one unique class, i.e., a single flow pattern in that set of data. The more transparent is a color, more flow patterns are in the dataset.

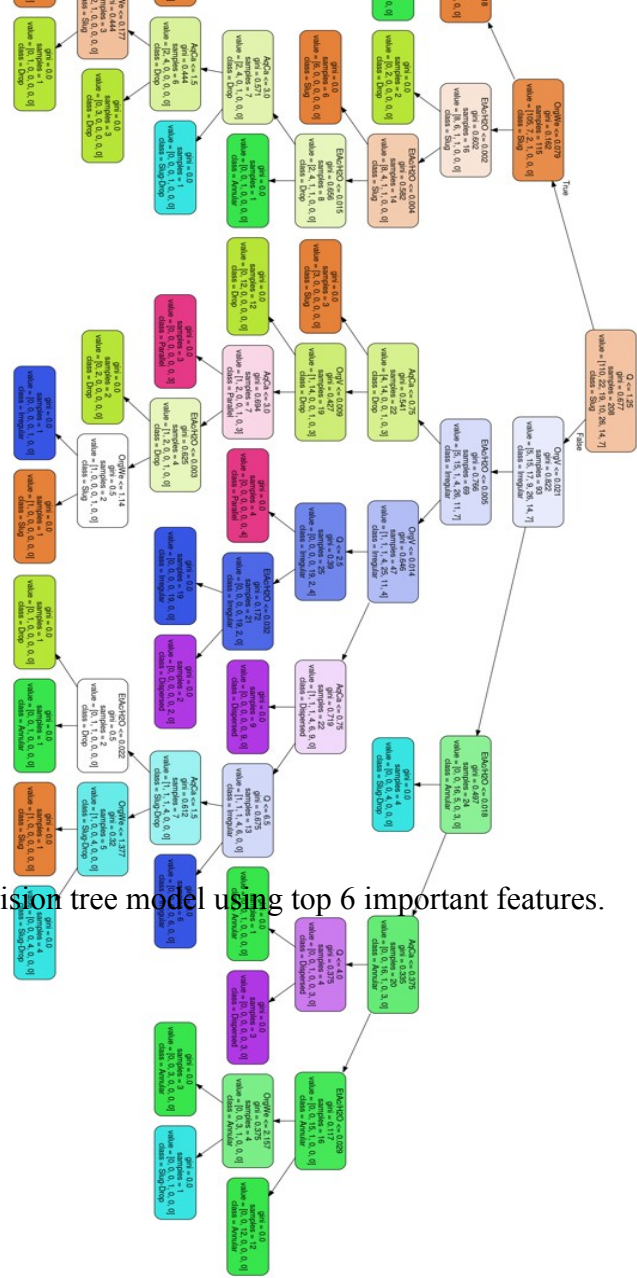


Figure S6. The full decision tree model using top 6 important features.